ORIGINAL ARTICLE

A method to analyze the evolution of malignant gliomas using MRI

**Maria Ida Iacono · Katia Passera ·
Lorenzo Magrassi · Luca Mainardi ·
Stefano Bastianello · Paolo Lago**

Abstract

Objective To introduce a novel approach for the monitoring of glioma evolution by the extraction of mathematical parameters from follow-up MRI.

Material and methods The method consists of the registration of follow-up MR images and the analysis of the deformation field. The registration was performed through an affine transformation followed by a non-rigid registration using free-form deformations (FFDs). A subsequent analysis of the transformation non-linear component is then performed by using the jacobian operator in order to extract information related to tumor evolution. In order to test the algorithm's performance two different validations were performed: (a) a numerical validation utilizing both physical and digital phantoms, (b) a clinical validation using neurosurgeon clinical judgements.

Results Quantitative validation showed that the jacobian describes the volumetric variations of the physical phantom with an error of 5%. Furthermore, simulations with a digital phantom provided an estimation of the error introduced by registration (6.4%). Clinical validation provided good clinical scores: the score evaluating the correspondence between extracted variables and patient evolution was 4.37 ± 0.89 for the deformation field and 4.43 ± 0.82 for the jacobian image (top score: 5).

Conclusion The novel approach leads to an objective and quantitative description of tumor evolution. Therefore, it could be valuable for planning interventions and/or treatments.

Keywords Computer-assisted image processing ·
Deformation field · Jacobian operator · Follow-up studies

M. I. Iacono · K. Passera · L. Mainardi (✉)
Biomedical Engineering Department, Politecnico di Milano,
Milan, Italy
e-mail: luca.mainardi@biomed.polimi.it

M. I. Iacono
e-mail: maria.iacono@mail.polimi.it

K. Passera
e-mail: katia.passera@polimi.it

L. Magrassi
Neurosurgery Division, Department of Surgery, IRCCS S. Matteo,
University of Pavia, Pavia, Italy
e-mail: l.magrassi@smatteo.pv.it

S. Bastianello
Department of Neuroradiology, IRCCS Mondino, Pavia, Italy
e-mail: stefano.bastianello@mondino.it

P. Lago
Clinical Engineering Department, IRCCS S. Matteo, Pavia, Italy
e-mail: lagop@smatteo.pv.it

Introduction

Neoplastic diseases of the central nervous system, particularly the glial ones, are highly lethal tumors. In fact, despite recent advances in conventional treatments, glioblastoma patients continue to have median survival outcomes of less than 18 months [1].

The high grade malignant gliomas require careful monitoring both during therapy and during follow-up for the evaluation of treatment effectiveness and for the early detection of a relapse.

In order to monitor tumor growth, magnetic resonance imaging (MRI) [2,3] is used. However there is a need for objective methods that provide for the quantification of changes in lesions. Change detection is an interesting investigation area of image processing: literature presents several

methods that aim to compare serial images in order to track disease modifications [4].

Visual inspection is certainly the simplest and most common approach for the analysis of pathology evolution when using MR images. Many approaches propose the subtraction of serial images in order to enhance the most relevant variations. This approach is obviously qualitative, however.

Another approach utilized to evaluate follow-up images is the assessment of tumor size.

In particular, the Response Evaluation Criteria in Solid Tumors, or RECIST criteria (one-dimensional [1D] measurement) are widely used to measure tumor response to therapy in clinical practice [5]. Although these methodologies represent an attempt to provide a reproducible and comparable evaluation method, they show many limitations including measurement subjectivity and high intra and inter-observer variability.

In addition, tumors may evolve in an irregular fashion and RECIST criteria may not be representative of the real growth.

Thus, radiologists sometimes manually outline lesions on images. Manual segmentation is more accurate but it is a time-consuming task. More automatic segmentation algorithms were developed in order to help clinicians with this task [6–10]. It should be noted that volume variation itself does not provide any information about the complex tumor growth pattern. Therefore, some authors have suggested the use of non-rigid registration/warping methods for the detection of changes. In particular, biomechanical physical models can be used [11,12] but they require the extraction of parameters related to mechanical tissue properties.

Recently a warping approach without constraints was proposed to automatically detect and segment the evolution of multiples sclerosis lesions [13].

In this paper a similar approach was implemented in order to analyze changes in gliomas during follow-up. First, images are aligned utilizing an affine registration. Then the displacement field is computed between images with a non-rigid registration based on B-splines. The analysis of this field by jacobian operator leads to the extraction of quantitative parameters that concisely describe the tumor growth.

The method was validated employing physical and digital phantoms and tested with a dataset of 15 patients.

Materials and methods

In this study the quantitative assessment of tumor growth is composed of two fundamental steps:

(1) a registration procedure to extract the deformation field;
(2) an analysis of the deformation field (implementing a jacobian operator) to describe tumor growth.

Registration procedure

Registration was performed using an approach proposed for dynamic contrast-enhanced MRI of the breast [14–16]. The algorithm is based on free-form deformations (FFDs) using B-splines and uses normalized mutual information (NMI) as a voxel-similarity measurement [17–19]. The main advantage of using NMI is that it makes no assumption on the relation between series image intensities and therefore it is the elective criterion when images show intensity and morphological differences due to different acquisition protocols and pathologies.

The algorithm models global patient motion using an affine transformation and subsequently models local motion by manipulating an underlying mesh of B-spline control points.

The flexibility and computational complexity of the local motion model is related to the choice of control point spacing.

Analysis of the deformation field

Once non-rigid registration between the target and the floating volume was performed, we derived a deformation field that describes pixel-by-pixel the displacement with respect to each control point (Fig. 1).

The jacobian operator was then applied to the deformation field in order to transform a 3D vector field into a 3D scalar image.

The jacobian operator was defined as the determinant of the jacobian matrix of the deformation field [20]:

$$\text{Jac}_\text{P}(\phi) = \det(\Delta_\text{P}\phi) = \begin{vmatrix} \dfrac{\partial\phi_x}{\partial x} & \dfrac{\partial\phi_x}{\partial y} & \dfrac{\partial\phi_x}{\partial z} \\[2mm] \dfrac{\partial\phi_y}{\partial x} & \dfrac{\partial\phi_y}{\partial y} & \dfrac{\partial\phi_y}{\partial z} \\[2mm] \dfrac{\partial\phi_z}{\partial x} & \dfrac{\partial\phi_z}{\partial y} & \dfrac{\partial\phi_z}{\partial z} \end{vmatrix}$$

This operator links the local variation $\frac{\delta V_\text{target}}{\delta V_\text{floating}}$ of an elementary volume δV_floating in the floating image to the corresponding warped volume δV_target in the target image:

$$\delta V_\text{target} = \text{Jac}_\text{P}(\phi) \cdot \delta V_\text{floating}$$

When $\text{Jac}_\text{P}(\phi) > 1$ there is a local expansion at the point P, while when $\text{Jac}_\text{P}(\phi) < 1$ there is a shrinkage at point P. The transformation locally preserves the volume when $\text{Jac}_\text{P}(\phi) = 1$.

It is worth noting that the integral of the jacobian represents the volume variation. Therefore, it can be used as an index of the degree of deformation of a particular region of interest.
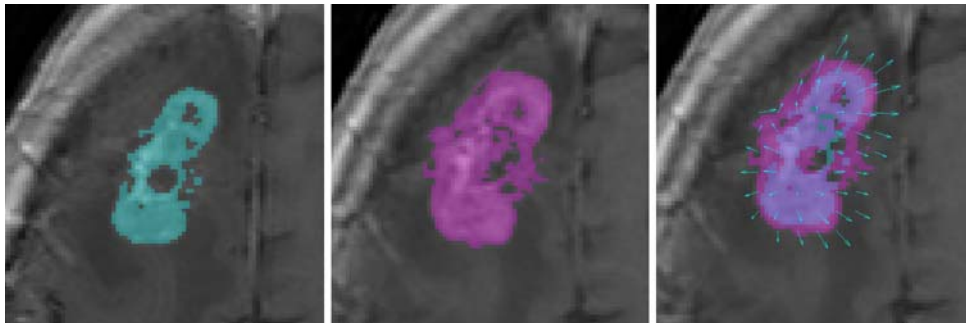
Fig. 1 Two images on the *left* MR transversal slices of a patient's brain at different times aligned by a 3D affine registration. In each data set the enhanced tumor area was manually segmented slice-by-slice by the neurosurgeon. Image on the *right* synchronous views of the lesion segmentation and the displacement field obtained by non-rigid registration

Workflow architecture

Figure 2 shows the algorithm workflow. The affine registration and the next non-rigid registration were performed with ITK (image registration toolkit) software [21].

After the affine registration, the registered volume, which is labelled as the intermediate floating volume, is stored. Next, the non-rigid registration between the intermediate floating volume and the target volume is performed and the non-rigid components of the vector field are isolated. These components are those related to the effective brain deformations. The jacobian operator is then applied to the resulted deformation field and its mean value is computed inside a volume of interest (VOI). The VOI is manually selected by the neurosurgeon using a graphical user interface (GUI) which visualizes simultaneously the registered volumes, the jacobian image and the jacobian mean value.

The jacobian image, obtained by mapping the result of the jacobian operator, is a visual instrument which permits the enhancement of areas with the most significant levels of deformation, while the mean jacobian represents a concise index of the degree of deformation.

The deformation field analysis and the GUI visualization were implemented using MATLAB software (MathWorks Inc., Natick, MA, USA).

Experimental protocol

Patient data

The algorithm was tested using an experimental protocol developed for post-surgery MRI studies.
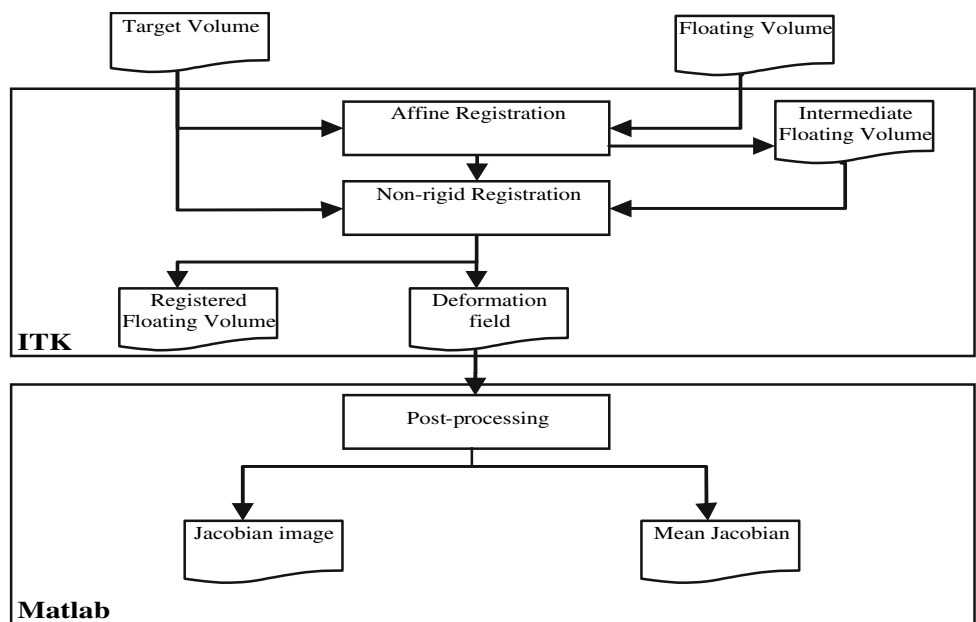
Fig. 2 The algorithm workflow

Fig. 3 *Top* axial slices of a digital phantom. The target phantom (*left*) with the known applied vector field (*middle*) and the floating warped phantom (*right*). *Bottom* the floating warped volume with increased enhancement (*left*), necrosis (*middle*) and edema (*right*)
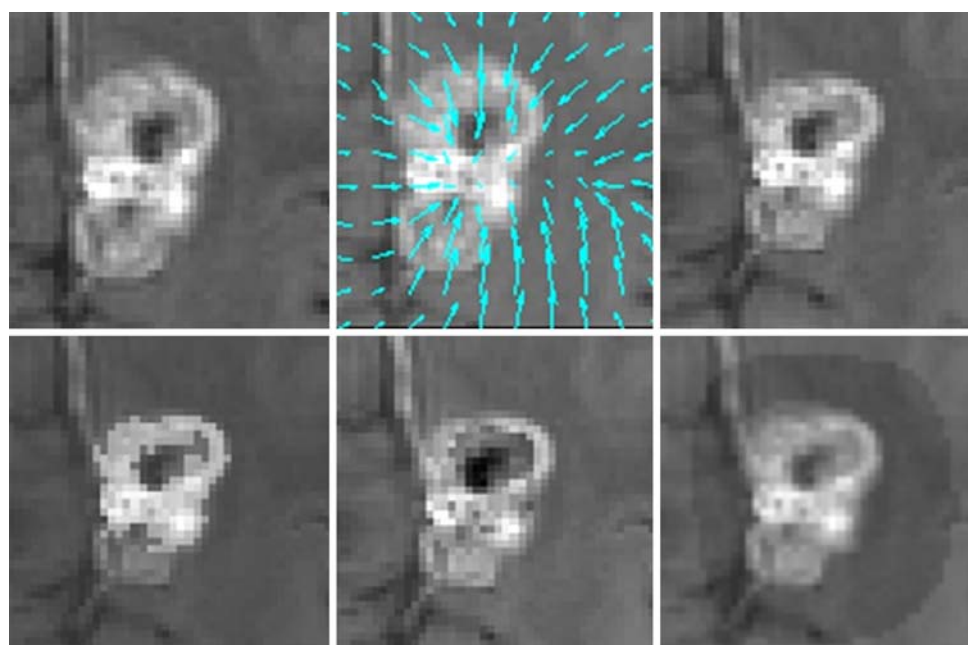

Table 1 Physical phantom results

Comparison (cc)	ΔV_r (%)	ΔV_j (%)	Error %	J_{mean}
24–39	62	58	6	1.68
39–59	51	55	7	1.61
24–59	145	131	9	2.27
59–59	0	−0.01	0	1.02

We examined 15 patients operated for gliomas. For each patient, 3 MRI volumes were acquired at different post-operation times as scheduled for follow-up.

All patients underwent 1.5 T MR imaging (Philips General System). Spin-Echo T1-weighted sequences (TR = 540.636 ms, TE = 15 ms, FLIP ANGLE = 90) were acquired (axial orientation) after contrast agent injection. The slice thickness was 6 mm with an inter-slice gap of 6.6 mm; the pixel size in axial plane was 0.894 mm × 0.894 mm.

Registration was computed on each pair of sequential MR image series: thus the second series was registered on the first and the third on the second.

Phantom data

The deformation of an endocranial tumor was mimicked with a phantom in order to evaluate the method reliability in quantifying volume changes. Using the phantom a four-phase protocol was defined. The phantom had a catheter inside. In this catheter a fixed amount of saline solution (24 cc) was injected (Phase 1). Next contrast agent was injected: an initial injection of 15 cc of gadolinium (Phase 2) was followed by an additional injection of 20 cc of contrast agent (Phase 3).

The first condition represented the basal situation, the second and the third represented the tumor growth and its contrast uptake. Finally the phantom was translated (1 cm) to simulate a misplacement error (Phase 4). In each of the four phases, a MR acquisition was performed. The acquisition was performed with a Siemens MRI system. Acquisition parameters (TR = 1,790 ms, TE = 3.93 FLIP ANGLE = 15°) were optimized to best enhance the image registration. We aimed especially at performing a sequence useful with an isotropic voxel (1.1 mm × 1.1 mm × 1.1 mm). This is an essential condition for good three-dimensional registration.

Simulated data

The proposed method was also tested on a digital phantom to assess the accuracy when implementing data with realistic complexity (tumor variability in size, appearance, and structure).

First of all a VOI containing a tumor was extracted from a patient MR scan. A new image volume was created. This volume, assumed as a target volume, was further spline-interpolated to create a high resolution volume with isotropic voxel dimensions of 1 mm.

Simulated shape changes (SC) were obtained applying known deformation fields on the phantom.

Four different deformation fields were applied on the target volume including incoming vector fields (IF, to simulate tumor shrinkage) and outgoing vector fields (OF, to simulate tumor growth). From an initial incoming vector field (IF1), three other fields were derived as follow: (a) by halving IF1 magnitude (IF1/2), (b) by inverting its direction (OF1) and

Fig. 4 *Top left and right* A slice of the target lesion and a slice of the floating lesion in their three transversal, frontal and sagittal projections. *Bottom left and right* The target lesion with its deformation field and the jacobian image
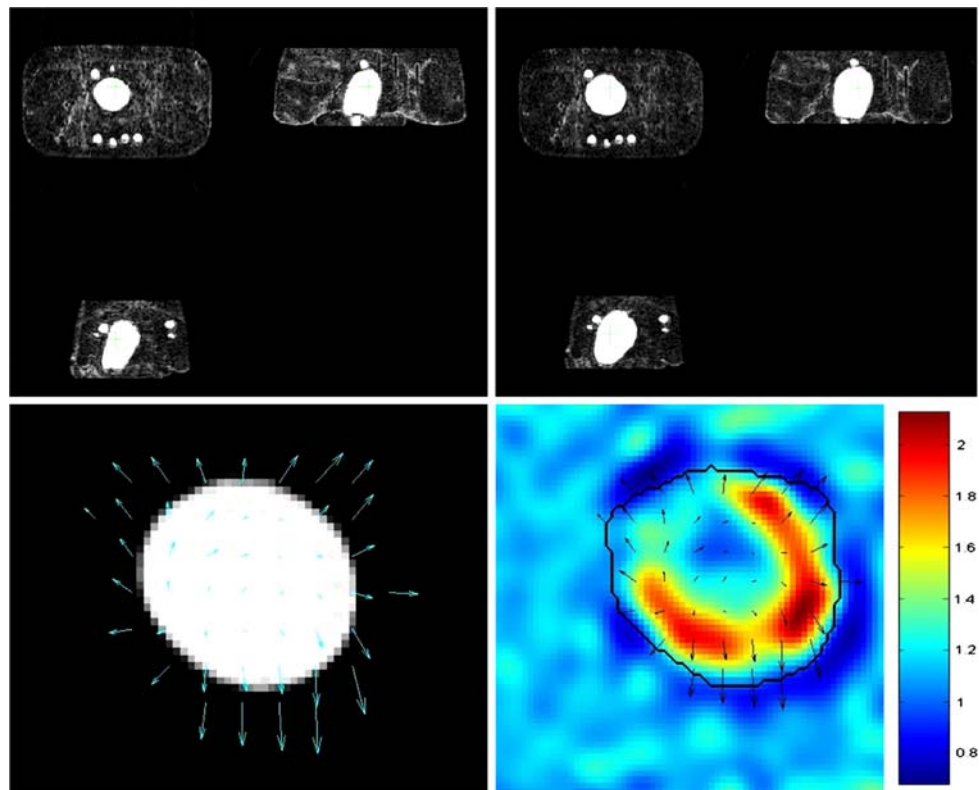
(c) by simultaneously halving the magnitude and inverting the direction (OF1/2).

In addition, in order to quantify the method performances under realistic conditions the voxels of the resulting warped volumes were modified to simulate both alterations in lesion composition (local Enhancement, EHN, and necrosis, NEC) and the development of peritumoral edema (ED).

The resulting four volumes (the warped volume and the modified ones), obtained for each vector field, were used as the floating volumes for the subsequent registration procedure (Fig. 3).

Results

Method validation was based on two different approaches: (1) a quantitative validation based on the use of physical and digital phantoms and (2) a clinical validation based on the qualitative analysis of the deformation field performed by the neurosurgeon.

Quantitative validation

Phantom data

We verified that the volumetric variation expressed by the jacobian operator ($\Delta V_j\%$) matched the real volumetric variation ($\Delta V_r\%$) imposed by the protocol.

An accurate segmentation of the catheter (tumor) was performed on the registered floating series. In this VOI, jacobian values were integrated in order to obtain $\Delta V_j\%$.

Table 1 shows that the jacobian is able to describe the real volumetric variations: in any comparison, the error (absolute value) is less than 10%.

In addition, the mean jacobian values (obtained in the VOI) were able to correctly identify volume expansions (jacobian > 1) and quantify them.

When the phantom was only translated we observed a value of the jacobian around 1 (as correctly expected). Higher values were observed when the concentration of the contrast agent was augmented (see Table 1). In particular, volume increments were correlated to mean jacobian values. For example, for a 62% real volume increment a 1.62 mean jacobian value would be expected. It is worth noting that the obtained values were close to the ideal ones.

Further, the jacobian mapping was able to enhance anisotropy in the deformation that occurred between step 2 (39 cc) and step 3 (59 cc) of the experiment (see Fig. 4 for details).

Simulated data

The target and the floating volumes were non-rigidly registered in order to estimate the vector fields able to detect tumor deformations.

Table 2 Digital phantom results

Field	Change	V_t (cc)	V_f (cc)	ΔV_k (cc)	ΔV_e (cc)	Error %
IF 1	SC	12.43	7.61	4.41	4.16	6
	SC + ENH			4.41	3.94	11
	SC + NEC			4.41	3.88	12
	SC + ED			4.41	3.84	13
IF 1/2	SC	12.43	10.01	2.08	2.04	2
	SC + ENH			2.08	1.98	5
	SC + NEC			2.08	2.01	3
	SC + ED			2.08	1.98	5
OF 1	SC	12.43	17.15	4.66	4.43	5
	SC + ENH			4.66	4.33	7
	SC + NEC			4.66	4.23	9
	SC + ED			4.66	4.25	9
OF 1/2	SC	12.43	14.98	2.39	2.45	2
	SC + ENH			2.39	2.55	7
	SC + NEC			2.39	2.46	3
	SC + ED			2.39	2.49	4

Table 3 The MME (mm) and MAE values (°) and their respective standard deviations (SD) between the known vector fields and the estimated ones

Field	Change	MME ± SD	MAE_a ± SD	MAE_z ± SD
IF 1	SC	0.014 ± 0.202	0.186 ± 4.448	0.260 ± 3.867
	SC + ENH	0.014 ± 0.207	0.185 ± 4.321	0.233 ± 3.539
	SC + NEC	0.015 ± 0.214	0.180 ± 4.233	0.224 ± 3.394
	SC + ED	0.014 ± 0.209	0.170 ± 4.063	0.242 ± 3.664
IF 1/2	SC	0.004 ± 0.060	0.117 ± 3.351	0.105 ± 1.720
	SC + ENH	0.004 ± 0.061	0.126 ± 3.545	0.103 ± 1.613
	SC + NEC	0.004 ± 0.058	0.129 ± 3.585	0.099 ± 1.587
	SC + ED	0.004 ± 0.061	0.104 ± 3.172	0.110 ± 1.837
OF 1	SC	0.009 ± 0.126	0.157 ± 3.929	0.114 ± 1.880
	SC + ENH	0.008 ± 0.122	0.175 ± 4.235	0.101 ± 1.719
	SC + NEC	0.009 ± 0.132	0.158 ± 3.938	0.130 ± 2.075
	SC + ED	0.011 ± 0.159	0.158 ± 3.909	0.184 ± 2.957
OF 1/2	SC	0.004 ± 0.054	0.137 ± 3.617	0.122 ± 2.169
	SC + ENH	0.004 ± 0.057	0.164 ± 4.103	0.124 ± 2.211
	SC + NEC	0.004 ± 0.064	0.149 ± 3.762	0.145 ± 2.528
	SC + ED	0.004 ± 0.057	0.140 ± 3.673	0.133 ± 2.497

Then, the known vector fields and the estimated ones were analyzed applying the jacobian operator.

The jacobian operator resulting from the known vector field was labelled known jacobian, while the jacobian operator extracted from the estimated one was labelled estimated jacobian.

Table 2 summarizes results obtained from the digital phantom simulations. The third and the fourth columns of Table 2 report the target (V_t) and floating volumes (V_f), as obtained by manual segmentation.

The known volume variation (ΔV_k) and the estimated one (ΔV_e) were obtained integrating the known and the estimated jacobian respectively. Integration was performed on a VOI as before.

The percentage error (Error %) provides an estimation of the errors introduced by the registration procedure in the

Fig. 5 The first two columns represent the different axial slices related to the two dates compared (*left* target volume, *middle* floating volume). The column on the *right* represents the different axial slices of the jacobian image and its value scale
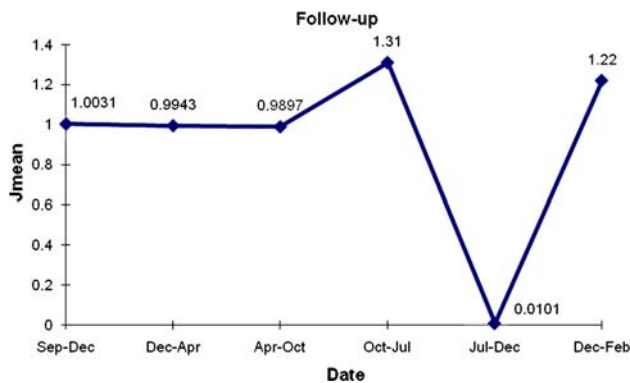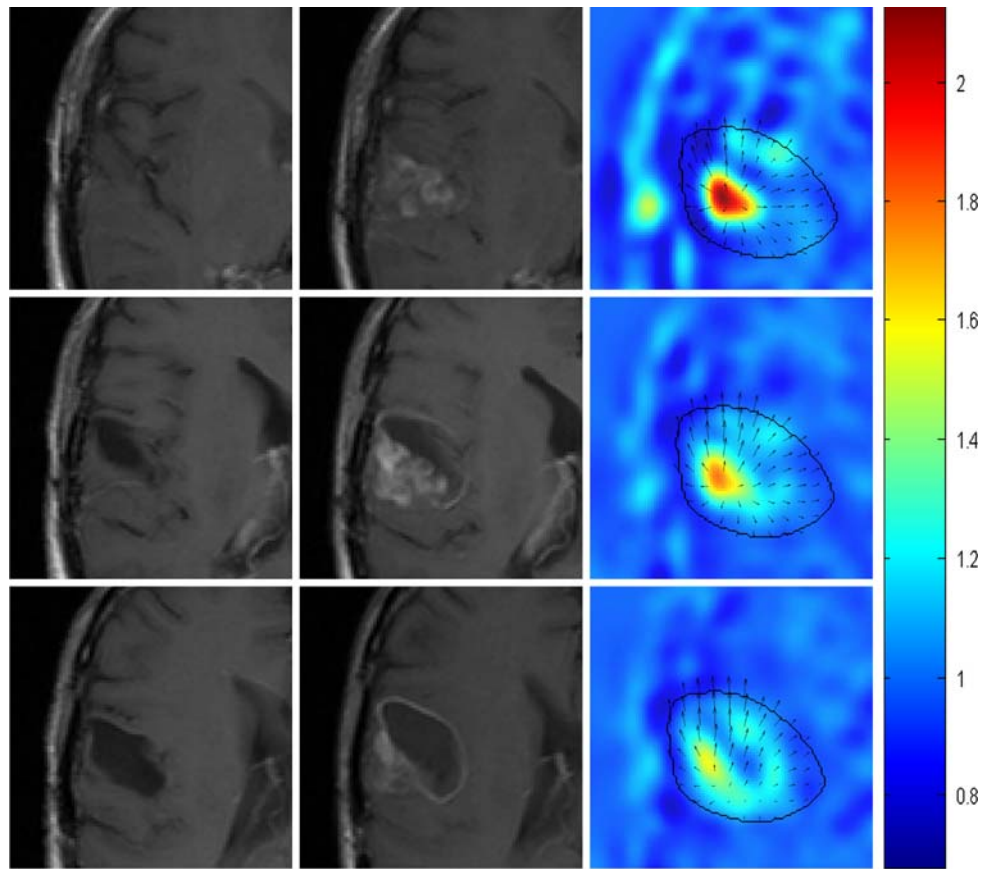

Fig. 6 Trend of the mean jacobian in function of the different comparisons

volumetric variation computation using the jacobian operator. The error values prove that the introduction of intensity modifications like enhancement, necrosis and edema do not significantly affect the performance of the algorithm in estimating volumetric variations. In fact, when intensity modifications were included, the volumetric deformation was estimated with a lightly larger error, Δe ($\Delta e = 6\%$ for IF1, $\Delta e = 2.3\%$ for IF1/2, $\Delta e = 3.3\%$ for OF1, $\Delta e = 2.7\%$ for OF1/2). Interestingly, the algorithm performs better with small deformations: when we halved the vector fields the error was lower than 7%.

For a quantitative comparison between the known vector fields $\mathbf{d(n)}$ and the estimated ones $\mathbf{s(n)}$ we have considered the mean magnitude error (MME) and the mean angular error (MAE) defined as:

$$\text{MME} = \overline{\|\mathbf{d(n)} - \mathbf{s(n)}\|}$$

$$\text{MAE} = \overline{\|\angle\mathbf{d(n)} - \angle\mathbf{s(n)}\|}$$

MAE was computed considering both the azimuth (MAE_a) and the zenith angles (MAE_z).

Table 3 demonstrates that the estimated vector fields, resulting from the registration procedure, are very close to the true ones. Error values are low and they do not increase significantly even if intensity changes occur. Again, better performances were achieved for subtler deformations, in agreement with the results obtained for the volumetric variation.

Clinical validation

The implemented method provides two main outputs: the deformation field and the jacobian image. To assess their clinical utility in describing tumor evolution we asked the neurosurgeon to score them on the basis of several different considerations. These considerations included the agreement of clinical analysis with respects to the usual clinical tools

(visual analysis of the images, analysis of the patient symptomology, disease course, and other related exams), their ability to summarize information, and their clarity and user-friendliness in terms of extracted information.

Scores range from 1 to 5 with 1 representing an "awful correspondence" and 5 an "excellent correspondence" with the actual state of the pathology.

For each output, mean scores were computed as the average of all patient scores. For each patient two comparisons were available. Therefore any output mean score was computed on a total of 30 values.

Both the deformation field and the jacobian image achieved high scores: 4.37 ± 0.89 (mean $\pm$ SD) and 4.43 ± 0.82, respectively.

Figure 5 shows for a patient three axial contiguous slices of the first series (first column) and of the subsequent series (second column). The third column shows the relative jacobian images obtained by the comparison between them.

Both of the series were executed post-surgery. It is worth noting the "vacuum" due to the tumor resection which is identifiable in the images.

In addition, the images show a pathology relapse and a consequent volumetric expansion, which is well characterized by the jacobian images and by its mean value (1.31).

In particular, for one patient, seven exams were performed in different stages of the disease yielding a total of six comparisons which allowed for an analysis over time of the disease progression.

Figure 6 shows the trend of the mean jacobian parameter in successive acquisitions. This parameter effectively summarizes the follow-up clinical information for the patient. In fact, the calculated parameter values for the periods from September/December, December/April and April/October are near 1 and correspond to a stationary state of the pathology.

In addition, the mean jacobian trend fits all of the other events well: the disease recovery between October and July, the disease regression between July and December (surgery in August) and the relapse after December.

Discussion

We have proposed a method for measuring tumor changes based on a 3D registration procedure followed by a morphological analysis of the resulting vector field.

Recently, similar techniques to analyze distribution of brain deformations caused by pathology were proposed to segment the areas corresponding to a significant time evolution in neurodegenerative diseases, such as Multiple Sclerosis. In [13] the jacobian operator was thresholded and used to detect and segment the areas that are interested by the pathology. Conversely, in our method the jacobian image is

used to obtain a concise parameter to quantify the degree of deformation of the lesion.

The registration algorithm was chosen for its general applicability, transparency and computational efficiency. It is based on a similarity measure that is independent of intensity variations between images. Consequently, it is versatile to process follow-up studies in which acquisition settings may be slightly changed. More detailed physical models could be used to model lesion growth but their computational expense is very high, especially when 3D data are considered. Furthermore, the creation of a discrete mechanical model can be difficult and time consuming and it requires identification and assignment of the respective tissue properties before registration. On the contrary, our algorithm makes no assumption about the underlying properties of the different tissue types in the brain.

Results confirmed that the information obtained from the jacobian of the deformation field may be useful to detect and quantify the volumetric variation in cerebral gliomas. The mean jacobian value was found to be a reliable descriptor of the pathology evolution, in agreement with clinical evaluations related to the symptomology and with the clinical reports.

The jacobian image was computed on the whole volume and this enabled for the study of other anatomical structures intrinsically related to the pathology due to their spatial proximity (e.g. the evaluation of the compression of the ventricles or of the surrounding tissues during a lesion expansion). This mapping is, therefore, much more informative than the extraction of a unique parameter, like the growth or the shrinking percentage of the tumor as obtainable by segmentation or RECIST methods.

Furthermore, although gliomas are mostly fast growing solid tumors, their growth pattern is not easily predictable. In fact, the actual tumor growth pattern is not easily fitted by any linear function, especially when tumors are subject to multi-modality treatments which profoundly perturb their growth. In this case RECIST criteria can not be fully representative of the observed modifications. This observation increases the importance of developing more articulate techniques to assess pathology evolution.

Study limitations

The study is retrospective and based on archival material of routine scans that are used in clinical practice for the follow-up of patients affected by malignant gliomas. As a consequence, the acquisition parameters for the real cases were not optimal for the registration procedure. Because of the elevated slice thickness (6 mm) we considered the components of the deformation field in the slice plane only. Only on them the jacobian operator was applied.

Furthermore, due to the retrospective nature of the study design some biases and inaccuracies resulted.

Besides artifacts intrinsically related to the jacobian operator (border effects at the edges), jacobian images of the real cases show artificial deformations due to registration errors. In fact, large slice thickness can induce a misalignment, generating false positive results.

Nevertheless, results are consistent with clinical judgments, showing the robustness and the versatility of the method for clinical routines even if a specific protocol has not been developed.

In addition, the method was also tested simulating the optimal conditions on physical and digital phantoms. Thanks to their voxel isotropy, they were processed on 3D basis, taking full advantage of the proposed approach and showing method reliability in detecting and quantifying tumor changes.

Future works

The obtained, preliminary results are encouraging, thus stimulating future work to fully exploit the method and its performances.

In our phantom data only spherical and homogeneous lesions were evaluated. It would be interesting to test the method using more realistic phantom, including asymmetric lesion growth or inhomogeneous intensities (mimicking edema, enhanced areas or necrotic areas, etc). In our study these aspects were evaluated through simulated digital data only.

In addition, we focused attention on post-surgery data and we limited the clinical evaluation to relapse quantification. In future works, we aim at evaluating the method in the monitoring of subtle tumor changes at short times intervals. This kind of analysis, that is more challenging for the human observers, would enable to assess the performance of the proposed method in comparison with visual inspection and to confirm the need of such a elaborate tool to support the physicians in their decisions. In this context, a more sophisticated registration framework which takes into account additional properties of the images/tissues, like the different intensity of the lesion or the modifications of the peritumoral areas, could be useful.

References

1. Quigley MR, Post C, Ehrlich G (2007) Some speculation on the origin of glioblastoma. Neurosurg Rev 30(1):16–20
2. Debnam JM, Ketonen L, Hamberg LM, Hunter GJ (2007) Current techniques used for the radiologic assessment of intracranial neoplasms. Arch Pathol Lab Med 131(2):252–260
3. Henson JW, Gaviani P, Gonzalez RG (2005) MRI in treatment of adult gliomas. Lancet Oncol 6(3):167–175
4. Patriarche J, Erickson B (2004) A Review of the Automated Detection of Change in Serial Imaging Studies of the Brain. J Digit Imaging 17:158–174
5. Padhani AR, Ollivier L (2001) The RECIST (response evaluation criteria in solid tumors) criteria: implications for diagnostic radiologists. Br J Radiol 74:983–986
6. Clark MC, Hall LO, Goldgof DB, Velthuizen R, Murtagh FR, Silbiger MS (1998) Automatic tumor segmentation using knowledge-based techniques. IEEE Trans Medical Imaging 17(2):187–201
7. Clarke LP, Velthuizen RP, Camacho MA et al (1995) MRI Segmentation: methods and applications. Magn Reson Imaging 13:343–362
8. Clarke LP, Velthuizen RP, Clark M et al (1998) MRI Measurement of brain tumor response: comparison of visual metric and automatic segmentation. Magn Reson Imaging 16:271–279
9. Ho S, Bullitt E, Gerig G (2002) Level set evolution with region competition: automatic 3-D segmentation of brain tumors. In: Proceedings of 16th International Conference on Pattern Recognition. IEEE Computer Society, Washington, pp 532–535
10. Liu J, Udupa JK, Hackney DC, Moonis G (2001) Estimation of tumor volume with fuzzy connectedness segmentation of MRI. Proc SPIE Med Imag 4322:1455–1465
11. Clatz O et al (2005) Realistic simulation of the 3D growth of brain tumors in MR images coupling diffusion with mass effect. IEEE Trans Medical Imaging 24(10):1334–1346
12. Kyriacou S et al (1999) Nonlinear elastic registration of brain images with tumor pathology using a biomechanical model. IEEE Trans Medical Imaging 18(7):580–592
13. Rey D, Subsol G, Delingette H, Ayache N (2002) Automatic detection and segmentation of evolving processes in 3D medical images: application to multiple sclerosis. Medical Image Anal 6(2):163–179
14. Denton ERE, Sonoda LI, Rueckert D, Rankin SC, Hayes C, Leach M, Hill DLG, Hawkes DJ (1999) Comparison and evaluation of rigid and non-rigid registration of breast MR images. J Comput Assist Tomogr 23:800–805
15. Rueckert D, Sonoda LI, Hayes C, Hill DLG, Leach MO, Hawkes DJ (1999) Non-rigid registration using free-form deformations: application to breast MR images. IEEE Trans Medical Imaging 18(8):712–721
16. Schnabel J, Rueckert D, Quist M, Blackall JM, Castellano Smith AD, Hartkens T, Penney GP, Hall WA, Liu H, Truwit CL, Gerritsen FA, Hill DLG, Hawkes DJ (2001) A generic framework for non-rigid registration based on non-uniform multi-level free-form deformations. In: Fourth Int Conf on Medical Image Computing and Computer-Assisted Intervention (MICCAI '01), pp 573–581, Utrecht, NL
17. Maes F, Vandermeulen D, Suetens P (2003) Medical image registration using mutual information. Proc IEEE 91(10):1699–1722
18. Pluim JP, Maintz JB, Viergever MA (2003) Mutual-information-based registration of medical images: a survey. IEEE Trans Med Imaging 22:986–1004
19. Viola P (1995) Alignment by maximization of mutual information. Ph.D. thesis, Massachusetts Institute of Technology
20. Davatzikos C, Vaillant M, Resnick S, Prince JL, Letovsky S, Bryan RN (1996) Morphological analysis of brain structures using spatial normalization. Vis Biomed Comput Lect Notes Comput Sci 1131:355–360
21. http://wwwhomes.doc.ic.ac.uk/~dr/software/download.html